Single Nanocrystal Arrays on Patterned Poly(ethylene glycol) Copolymer Microstructures Using Selective Wetting and Drying

Kahp Y. Suh,*,† Ali Khademhosseini,‡ George Eng,§ and Robert Langer*,‡,§

School of Mechanical and Aerospace Engineering, Seoul National University, Seoul 151-742, Korea, and Department of Chemical Engineering and Division of Biological Engineering, Massachusetts Institute of Technology, Cambridge, Massachusetts 02139

Received March 25, 2004. In Final Form: May 13, 2004

Single nanocrystal arrays were fabricated on sub-microwells of poly(ethylene glycol) (PEG) copolymer using selective wetting on the hydrophilic regions of the exposed substrate surface and subsequent drying. Templates were produced by molding a thin film of a PEG-based random copolymer on hydrophilic substrates such as glass or silicon dioxide. The polymeric microstructures provide a topographical barrier around the well, which makes it possible to create nanocrystal arrays with controlled geometrical features. The size of the nanocrystal was found to decrease with decreasing well size and also decrease with decreasing topological height. A simple empirical equation was derived to predict the size of the crystal as a function of the pattern size and height, which is in good agreement with the experimental data.

Introduction

Most successful fabrication of nanoparticle arrays involves crystal growth on or within well-defined two-dimensional (2D) or confined three-dimensional (3D) structures. The structures are mainly used as templates to guide the crystal nucleation and growth, allowing for various sizes and shapes. A number of templates have been employed including long chain organic monolayers,[1,2] bimineralized micellar solvents,[3−5] porous aluminum oxide,[6,7] polymeric matrix,[8,9] porous silicon,[10] carbon nanotube,[11] and highly ordered graphite.[12,13] Of these templates, the functionalized surface of self-assembled monolayers (SAMs) has been proven to be effective for successful crystal growth and patterning in comparison to other Langmuir monolayers or functionalized polymer surfaces.[14−17] Typically, highly ordered structures of SAMs of alkanethiolates on gold or silver surfaces have been extensively studied to selectively position nanoparticles on the hydrophilic regions.

Here, we present an alternative template-based method to fabricate nanocrystal arrays that utilizes the different wettabilities between the exposed substrate and the polymeric coating of a patterned surface. To provide a polymer template, we used a simple molding technique called capillary force lithography, which has been developed for patterning polymers on large areas.[18] When a mobile film is coated on a substrate while in conformal contact with a patterned poly(dimethylsiloxane) (PDMS) stamp, the capillarity forces the solution into the features of the stamp, thereby leading to the negative replica of the stamp. For the polymer, we used a poly(ethylene glycol (PEG)-based random copolymer, poly(3-trimethoxysilyl)-propylmethacrylate-*r*-poly(ethylene glycol) methyl ether [poly(TMSMA-*r*-PEGMA)]. This polymer contains surface-reactive trimethoxysilyl groups as a part of its backbone, which allows for the formation of multivalent bonds onto oxide surfaces, as well as multiple PEG chains. Detailed information on the synthesis and characterization of the polymer has been published elsewhere.[19]

Experimental Section

Fabrication of PDMS Stamps. PDMS stamps were fabricated by casting PDMS (Sylgard 184 elastomer, Essex Chemical) against silicon masters prepared by photolithography (1:10 ratio of the curing agent). Then the pre-polymer was well mixed and incubated at 75 °C for 1 h. After curing, PDMS stamps were detached from the master and cut prior to use.

Molding and Dipping into a Crystal Solution. A few drops of a 1−10 wt % solution of poly(TMSMA-*r*-PEGMA) in ethanol were placed on a glass or silicon dioxide wafer, and a thin film

* Corresponding author. Phone: +82-2-880-9103 (K.Y.S.); 617-253-3107 (R.L.). Fax: +82-2-883-0179 (K.Y.S.); 617-258-8827 (R.L.). Email: sky4u@snu.ac.kr (K.Y.S.); rlanger@mit.edu (R.L.).

† School of Mechanical and Aerospace Engineering, Seoul National University.

‡ Division of Biological Engineering, Massachusetts Institute of Technology.

§ Department of Chemical Engineering, Massachusetts Institute of Technology.

(1) Yang, J. P.; Meldrum, F. C.; Fendler, J. H. *J. Phys. Chem.* **1995**, *99*, 5500.
(2) Feng, S.; Bein, T. *Nature* **1994**, *368*, 834.
(3) Peng, X. G.; Manna, L.; Yang, W. D.; Wickham, J.; Scher, E.; Kadavanich, A.; Alivisatos, A. P. *Nature* **2000**, *404*, 59.
(4) Bekele, H.; Fendler, J. H.; Kelly, J. W. *J. Am. Chem. Soc.* **1999**, *121*, 7266.
(5) Li, Y. D.; Liao, H. W.; Ding, Y.; Qian, Y. T.; Yang, L.; Zhou, G. E. *Chem. Mater.* **1998**, *10*, 2301.
(6) Routkevitch, D.; Bigioni, T.; Moskovits, M.; Xu, J. M. *J. Phys. Chem.* **1996**, *100*, 14037.
(7) Sander, M. S.; Tan, L. S. *Adv. Funct. Mater.* **2003**, *13*, 393.
(8) Lin, J.; Cates, E.; Bianconi, P. A. *J. Am. Chem. Soc.* **1994**, *116*, 4738.
(9) Shin, K.; Leach, K. A.; Goldbach, J. T.; Kim, D. H.; Jho, J. Y.; Tuominen, M.; Hawker, C. J.; Russell, T. P. *Nano Lett.* **2002**, *2*, 933.
(10) Fan, S. S.; Chapline, M. G.; Franklin, N. R.; Tombler, T. W.; Cassell, A. M.; Dai, H. J. *Science* **1999**, *283*, 512.
(11) Han, W. Q.; Fan, S. S.; Li, Q. Q.; Hu, Y. D. *Science* **1997**, *277*, 1287.
(12) Gorer, S.; Ganske, J. A.; Hemminger, J. C.; Penner, R. M. *J. Am. Chem. Soc.* **1998**, *120*, 9584.
(13) Walter, J. *Adv. Mater.* **2000**, *12*, 31.
(14) Qin, D.; Xia, Y. N.; Xu, B.; Yang, H.; Zhu, C.; Whitesides, G. M. *Adv. Mater.* **1999**, *11*, 1433.
(15) He, H. X.; Zhang, H.; Li, Q. G.; Zhu, T.; Li, S. F. Y.; Liu, Z. F. *Langmuir* **2000**, *16*, 3846.
(16) Chen, C. C.; Lin, J. J. *Adv. Mater.* **2001**, *13*, 136.
(17) Lee, I.; Han, S. W.; Lee, S. J.; Choi, H. J.; Kim, K. *Adv. Mater.* **2002**, *14*, 1640.
(18) Suh, K. Y.; Kim, Y. S.; Lee, H. H. *Adv. Mater.* **2001**, *13*, 1386.
(19) Jon, S. Y.; Seong, J. H.; Khademhosseini, A.; Tran, T. N. T.; Laibinis, P. E.; Langer, R. *Langmuir* **2003**, *19*, 9989.

10.1021/la049217n CCC: $27.50
Published on Web 06/19/2004

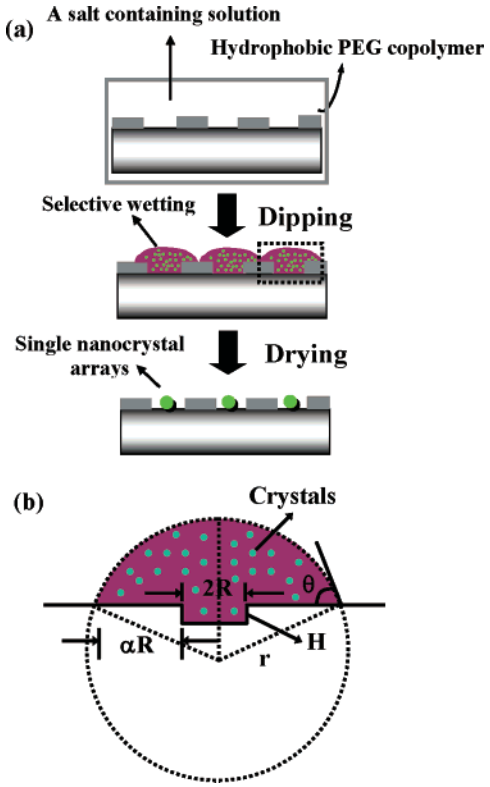

Figure 1. (a) Schematic illustration of the experimental procedure. (b) An illustration to depict the wetting of a drop around the exposed glass region.

of the copolymer was obtained by spin coating (model CB 15, Headaway Research, Inc.) at 1000 rpm for 10 s. To make conformal contact, PDMS stamps were carefully placed onto the surface and the samples were stored overnight at room temperature to allow for evaporation of the solvent. Four different well sizes were used (1000, 800, 700, and 500 nm) with the film thickness ranging from 34 to 610 nm after solvent evaporation, as determined by ellipsometry (Gaertner L116A, Gaertner Scientific Corp.) and atomic force microscopy (AFM). The patterned samples were dipped into a 1−3 M NaCl, Na_2CO_3, or Na_2SO_4 (granular) solution for 20 s and then withdrawn slowly. The samples were left undisturbed for a period of time until the solvent evaporated completely.

AFM. AFM images were taken in tapping mode on a NanoScope III Dimension (Veeco Instruments, Inc.) in air. The scan rate was 0.5 Hz, and 256 lines were scanned per sample. Tapping mode tips, NSC15, 300 kHz, were obtained from MikroMasch (Portland). Data were processed using Nanoscope III 4.31r6 software (Veeco Instruments, Inc.). Some of the images were flattened but not further manipulated.

Scanning Electron Microscopy (SEM). Images were taken using a high-resolution scanning electron microscope (JEOL 6320FV, MIT) at an acceleration voltage of 3 eV and a working distance of 7 mm. Samples were coated with a 30-nm Au layer prior to analysis to prevent charging.

Contact Angle Measurements. A Ramé-Hart goniometer (Mountain Lakes) equipped with a video camera was used to measure the static contact angles on drops of ~3 μL in volume. Reported values represent averages of at least three independent measurements.

Results and Discussion

Figure 1a outlines the procedure. In the experiment, templates were created on hydrophilic substrates such as glass or silicon oxide by molding a thin liquid film of the polymer. During the molding procedure, the substrate surface is completely exposed because of strong repulsion at the water/PDMS stamp while providing a different height of the microstructure depending on the initial polymer concentration and the geometry of the stamp.[20] Interestingly, as a result of the presence of trimethoxysilyl groups the polymer is slightly hydrophobic upon drying with the water contact angle of 60.7° in comparison to 2.3° for oxygen plasma-treated glass surface or 4.7° for the bare silicon dioxide surface. Nevertheless, the polymer still can absorb a certain amount of water as a result of the presence of PEG groups, which enables the selective wetting of a salt solution around the exposed regions. If conventional photoresists were used, loading the solution into the wells would be extremely difficult because of the capillary effect.

When the patterned substrate is immersed in an aqueous solution of an inorganic salt and then withdrawn, the solution wets and is retained selectively on the hydrophilic regions of the surface (i.e., exposed substrate).[21] It appears that the wetting extends to the adjacent regions because PEG is able to absorb water (Figure 1b). With time, water evaporates resulting in the shrinkage of the droplet size eventually leading to salt precipitation to form regular nanocrystal arrays within the confining 3D sub-microwells.

Figure 2 shows SEM and AFM images of arrays of the NaCl nanocrystal for various heights and sizes of the microstructures. In the experiment, four different well sizes were tested (1000, 800, 700, and 500 nm). Because of the limitation in the preparation of the stamp, we were not able to go below 500 nm. It was observed that the size of the nanocrystal decreases with decreasing well size and also decreases with decreasing topological height. Figure 2a−c shows large-area views of an 800 nm circular well with side wall heights of 195, 137, and 14 nm, respectively, whereas Figure 2d−f shows the corresponding enlarged views. As shown in the figure, the nanocrystal arrays are well-defined over large areas with the size ranging from 810 to 54 nm for a 1 M solution in water. The crystal arrays were more homogeneous and uniform for the 195-nm height with the density of 95 ± 3% (100% indicates no void wells after drying), decreasing monotonically to 67 ± 7% for the 14-nm height. This may be attributed to the difficulty in the preparation of the uniform microstructures for lower heights and nonhomogeneity of the initial pattern. A similar trend was observed for the other well sizes. In this regard, it should be possible to prepare ordered 2D arrays with lateral dimensions smaller than 50 nm using patterns with smaller feature sizes or salt solutions with lower concentrations. However, capillary effects may come into play as the well size decreases to a certain limit (e.g., trapping bubbles in the wells), which might hinder the successful loading of the solution into the wells. We hypothesize that the capillary effects would be circumvented by using a more hydrophilic polymer than PEG used in the experiment, which in turn decreases the difference in wettability.

In addition to changing the solution concentration and size of the microstructure, a different height gives rise to a different crystal size, suggesting that the liquid volume that can be contained in each "vessel" is directly proportional to the volume of the container. It is expected that the exact location of the crystal within the well could be determined by the initial uniformity of the pattern and physical parameters such as interfacial tension and withdrawing velocity and orientation.[22]

(20) Suh, K. Y.; Langer, R. *Appl. Phys. Lett.* **2003**, *83*, 1668.
(21) Kumar, A.; Biebuyck, H. A.; Whitesides, G. M. *Langmuir* **1994**, *10*, 1498.
(22) Maenosono, S.; Okubo, T.; Yamaguchi, Y. *J. Nanopart. Res.* **2003**, *5*, 5.

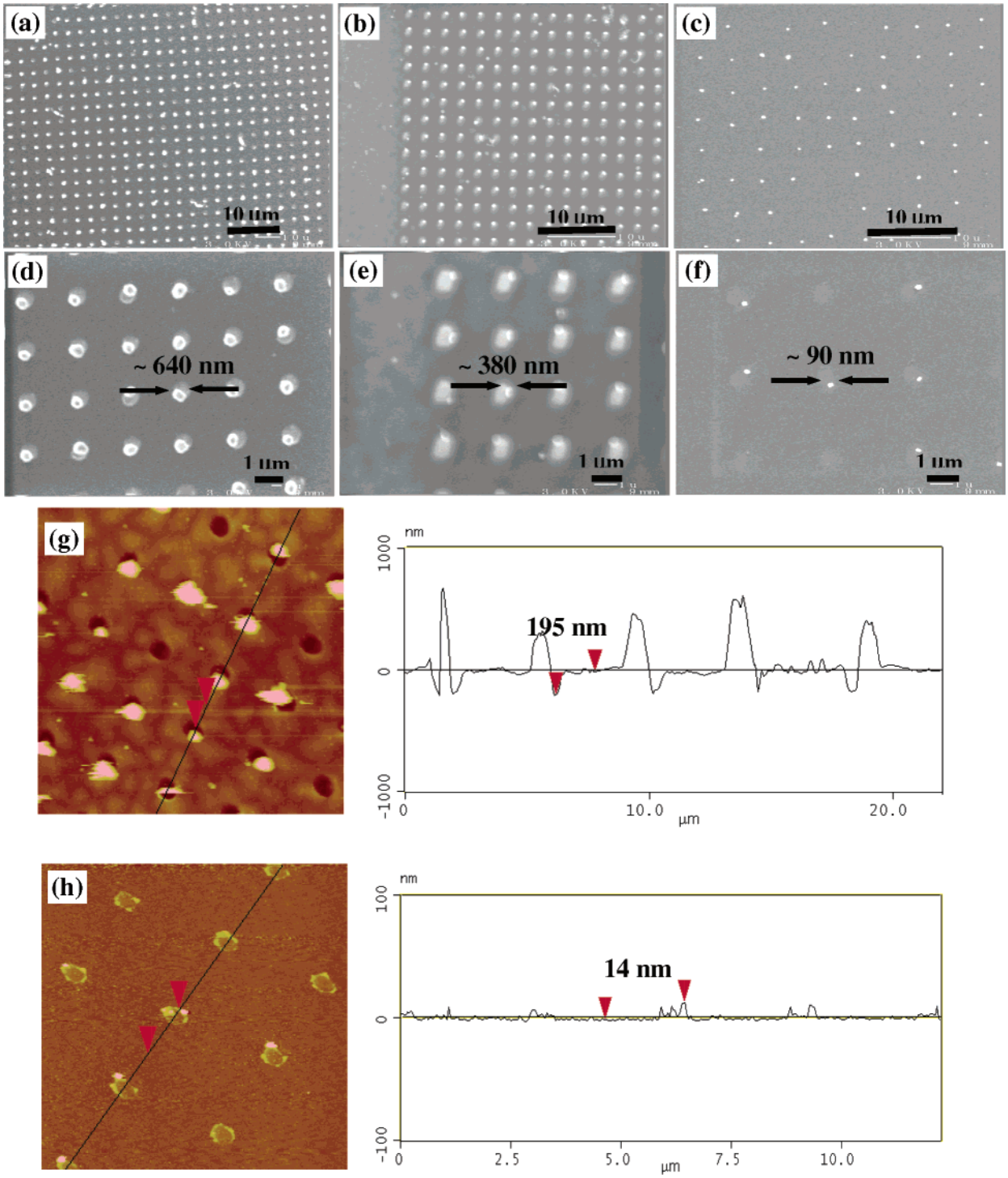

Figure 2. (a−c) SEM images for large-area views of nanocrystal arrays on 800-nm circular wells with different heights. (d−f) Enlarged views of the corresponding images in parts a−c. (g,h) Planar and cross-sectional AFM images for parts a and c, respectively. The scan size is 20 × 20 μm^2 for part g and 10 × 10 μm^2 for part h.

The current approach has a number of potential advantages over other lithographic or template-based methods including possible low cost and the ability to create microstructures with good fidelity over large areas. The PEG copolymer is biocompatible and nonbiofouling such that the method could be directly applied to biological applications involving nanoparticle-based sensors and detectors.[23] Alternatively, microcontact printing of SAMs has been successfully used to generate nanocrystal arrays.[14−17] The use of the technique, however, might be limited in that specific substrates such as gold or silver are necessary and the technique seems suitable for only a small number of material systems. In contrast, our method could be expanded to other hydrophilic substrates (e.g., metal oxides, polymers through oxygen plasma treatment if necessary) as long as the contact angle difference is large enough to provide selective wetting and drying. Moreover, different size nanocrystals can be fabricated at a given feature size using different heights, providing a flexible way of applying the technique.

(23) Khademhosseini, A.; Jon, S.; Suh, K. Y.; Tran, T. N. T.; Eng, G.; Yeh, J.; Seong, J.; Langer, R. *Adv. Mater.* **2003**, *15*, 1995.

To gain an understanding for the underlying mechanism, we calculated the size of the nanocrystal as a function of pattern size and height at a given concentration. Figure 1b shows a schematic illustration for the calculation geometry where θ is the contact angle, R and r are the radii of the well and the drop, respectively, H is the height, and α is the parameter indicating the degree of wetting outside the well. For convenience, we assume that all the salt is converted into the crystal (i.e., no salt is left behind as the drop dries) and only one spherical crystal is formed upon drying within a well. This assumption is valid for relatively low concentrations (<1 M) and slow evaporation. For higher concentrations and a fast evaporation rate, surface nucleation and crystal growth increases accordingly, such that the ordering of the crystals would be lost (data not shown). After manipulation of simple geometric consideration, the following is obtained

$$R_c = \left(\frac{c}{\rho_c}\right)^{1/3}\left[f(\theta)(1+\alpha)^3 + 0.75\frac{H}{R}\right]^{1/3} R \qquad (1)$$

where R_c is the radius of the crystal, c is the solution concentration, ρ_c is the density of the crystal, and $f(\theta) \equiv [(\theta/\pi)\ \mathrm{cosec}^3\ \theta - 0.75\ \cot\ \theta)$. For $H/R \ll 1$ (small aspect ratio),

$$R_c = \left(\frac{c}{\rho_c}\right)^{1/3}[f(\theta)]^{1/3}(1+\alpha)R \approx 0.13(1+\alpha)R \qquad (2)$$

where we used $\theta = \pi/3$, $c = 58.46$ g/cm^3, and $\rho_c = 2.16$ g/cm^3 for a 1 M solution of NaCl crystal. Equation 2 indicates that the crystal radius would be reduced to 13% of the radius of the well if there is no wetting on the polymer region ($\alpha = 0$). As shown in Figure 2, the radius of the crystal is typically larger than R_c when calculated with $\alpha = 0$, suggesting the wetting extends on the polymer region to a certain level. It is expected that the value of α would be reduced for highly hydrophobic polymers. Interestingly, α converges to 0 as the barrier height becomes small (e.g., 14 nm in Figure 2) so that one can obtain

$$R_c \approx \left(\frac{c}{\rho_c}\right)^{1/3}\left[f(\theta) + 0.75\frac{H}{R}\right]^{1/3}$$

$$R = 0.3\left(0.08 + 0.75\frac{H}{R}\right)^{1/3} R \qquad (3)$$

Thus, there is a critical aspect ratio below which α is assumed to be zero. We hypothesize that the critical aspect ratio is related to the meniscus formation within the well. If the well is sufficiently high to form a fully developed meniscus,[24] wetting is facilitated and further extends to the adjacent polymer surfaces. If the well is low, on the other hand, the meniscus breaks down as a result of mass depletion so that the solution might only wet the exposed glass region. In an extreme case, the drops could form locally at the corners of the well ($\alpha < 0$) and then one can observe one or two nanocrystals, which is in good agreement with the experimental result (Figure 2h). The critical aspect ratio can be determined by a simple geometric consideration, which gives[24]

$$\left(\frac{H}{R}\right)_c = \frac{1-\sin\theta}{\cos\theta} = 0.27 \qquad (4)$$

For example, the critical height is about 107 nm for an 800-nm circular well.

(24) Suh, K. Y.; Yoo, P. J.; Lee, H. H. *Macromolecules* **2002**, *35*, 4414.

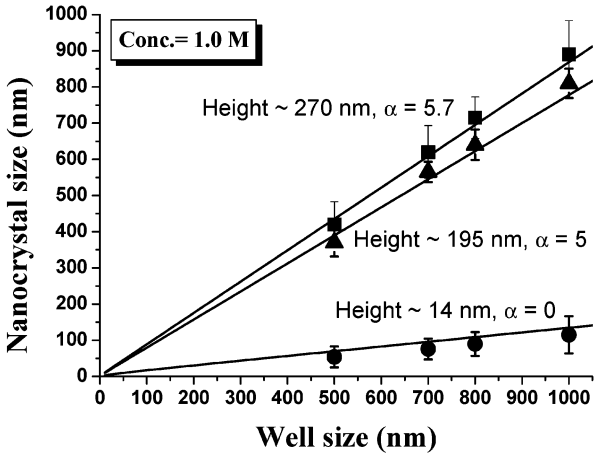

Figure 3. Comparison of the nanocrystal size between the calculation and the experimental data as a function of the pattern size and height. Note that α converges to 0 below the critical aspect ratio as given in the text.

Figure 3 shows a comparison between the prediction in eq 1 and the experimental data for various pattern sizes and heights. As seen from the figure, the data were in good agreement with the theory for the feature sizes tested.

Another possible advantage of the current method is that the PEG microstructures can guide the deposition of nanocrystal rods by using a line pattern and a high concentration. Figure 4 shows an example of the fabrication of NaCl rods using an 800-nm line-and-space pattern (Figure 4c,d) along with a typical example of nanodots within the lines (Figure 4a,b). For 1 M or lower concentrations, nanocrystal dots were sporadically formed within the channels without much ordering as shown in Figure 4a,b, the behavior of which is similar to nanocrystal arrays for circular wells with different barrier heights as described previously. As the concentration increases (>2 M), however, nanocrystals start to precipitate and merge, forming a dense rod along the channel direction (Figure 4b). The cross-sectional SEM image in Figure 4d shows that the PEG microstructures act to guide the patterned precipitation and the anisotropic growth of the crystal rods. Although the pattern fidelity is not as high as that for nanodot arrays presumably due to one-dimensional confinement, the method presented here could open a way to microengineering the shape of nanocrystals. Therefore, it may be possible to fabricate sharp needles or tips by inducing crystal growth within patterns specifically designed as negative imprints of the tips. In addition to NaCl crystals, we also tested other inorganic salts including Na_2CO_3 and Na_2SO_4 as shown in Figure 4e,f. As expected, different microstructures were observed depending on each type of crystal; NaCl crystals showed dense microstructures whereas Na_2CO_3 and Na_2SO_4 crystals showed porous and granular microstructures, respectively. Although not shown, a similar trend was observed for nanodot arrays regardless of the type of inorganic salt.

In summary, we have developed a simple and yet versatile method for fabricating nanocrystal arrays using selective wetting and drying. It was shown that the size of the nanocrystal can be controlled with different barrier heights, providing a flexible and versatile way of templating the crystal growth. Also, we derived a simple equation to predict the size of the crystal as a function of the pattern size and height. Also, the anisotropic formation of the nanocrystal was demonstrated using a line-and-space pattern, which is potentially useful for forming

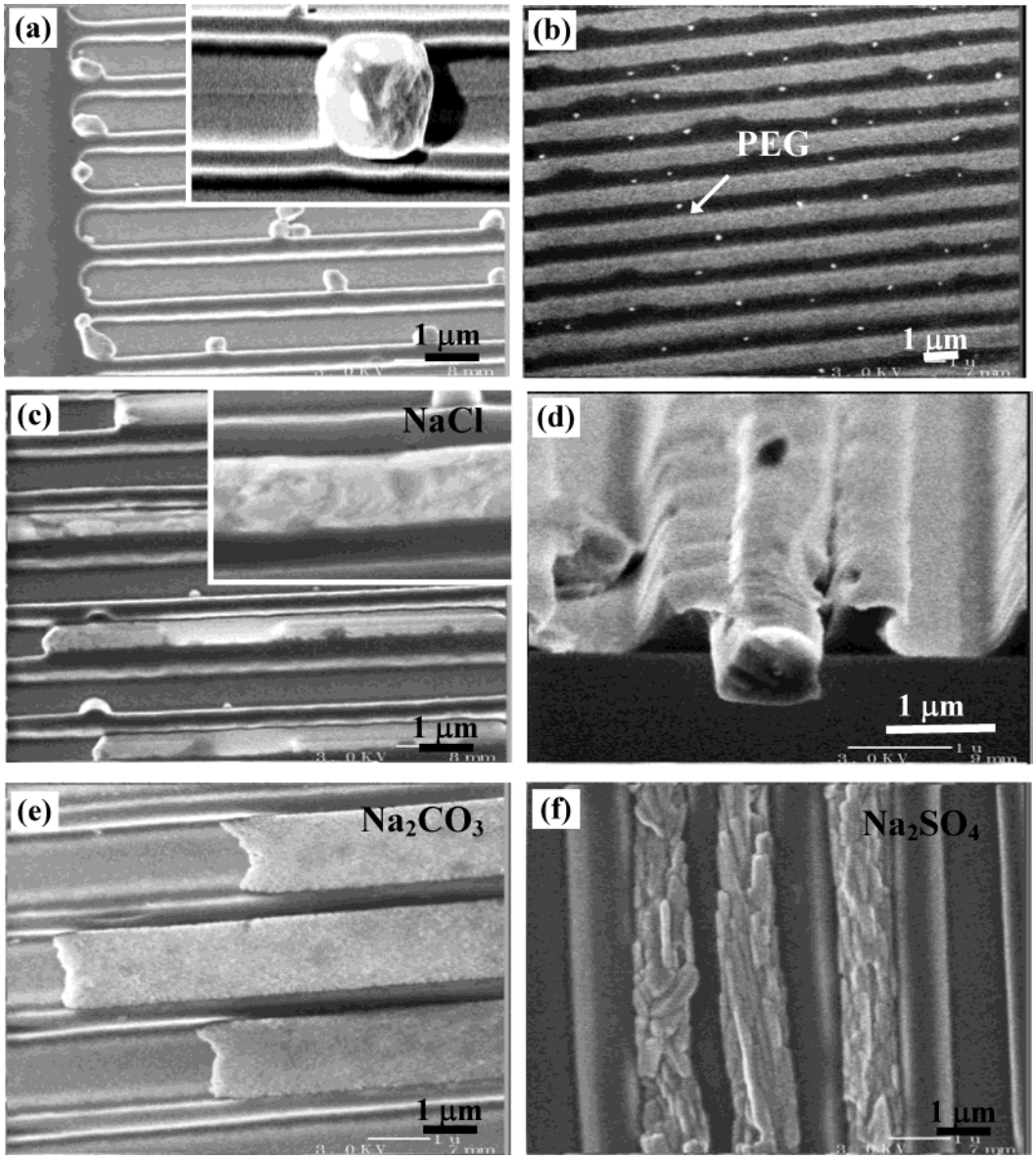

Figure 4. (a,b) SEM images for typical nanocrystal dot arrays formed within a channel with different barrier heights (275 nm for part a and 21 nm for part b, respectively). (c) A SEM image for nanocrystal rods formed along the channel direction. (d) A cross-sectional SEM image of the nanocrystal rods in part c. (e,f) SEM images for nanocrystal rods using different solutions.

nanocrystal rods. Although inorganic salts were used throughout the experiment as a model crystal, the method presented here could also provide routes to arrays of other simple organic or functionalized crystals with appropriate chemical reactions.

Acknowledgment. This research was supported by, or supported in part by, the U.S. Army through the Institute for Soldier Nanotechnologies, under Contract No. DAAD-19-02-D0002 with the U.S. Army Research Office. K.Y.S. was also supported by Brain Korea 21 in 2004. The authors thank Dr. Sangyong Jon for providing the PEG copolymer and Dr. Hongming Chen for helpful discussions.

LA049217N